# NLO corrections to WWZ and ZZZ production at the ILC

LE Duc Ninh

ldninh@mppmu.mpg.de

Max-Planck-Institut für Physik
(Werner-Heisenberg-Institut)

**Based on Fawzi Boudjema, LDN, Sun Hao, Marcus Weber, Phys.Rev.D81:073007,2010.**

*CPP 2010, Sep 24, KEK.*

# Outline

- Motivation
- Calculations: $e^+e^- \to ZZZ, WWZ$
- Numerical results
- Conclusions

# The SM

LEPEWWG 2010:

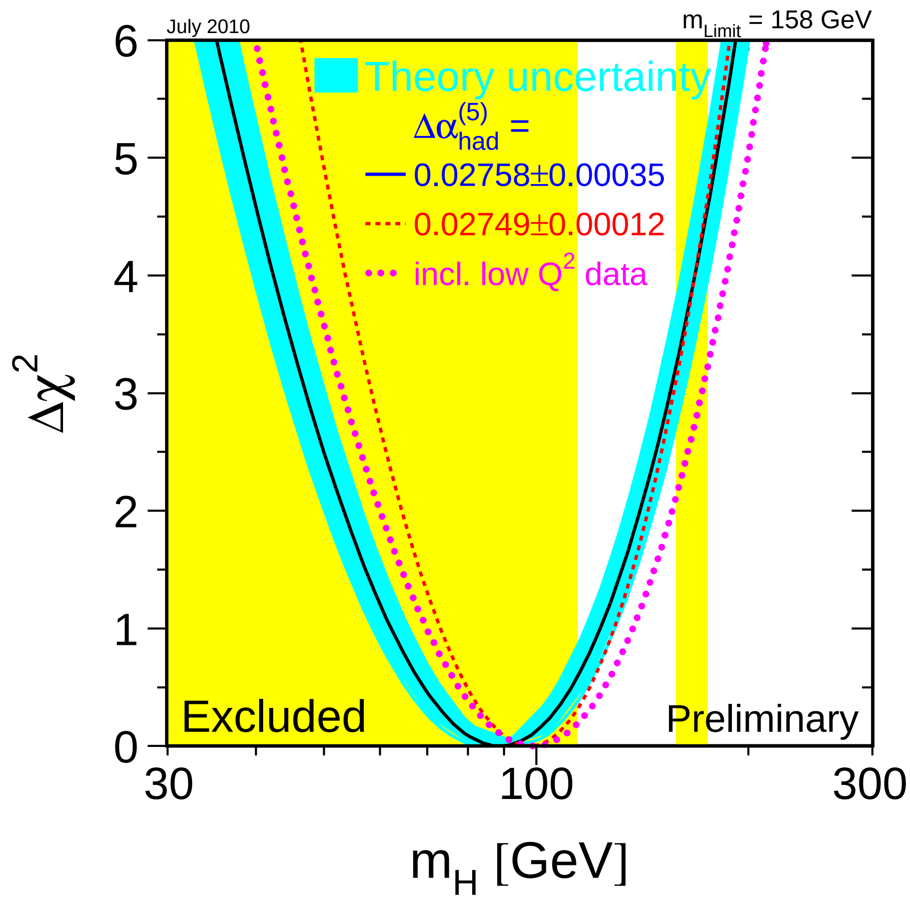


- LEP direct search ($e^+e^- \nrightarrow ZH$, $\sqrt{s} = 209$GeV): $M_H > 114$GeV
- CDF and D0 $p\bar{p} \nrightarrow H \to W^+W^-$: $M_H \notin [158, 175]$GeV.
- Precision EW measurements: $\to M_H < 158$GeV ($\Delta\chi^2 = 2.7$).

# SM trilinear and quartic gauge couplings

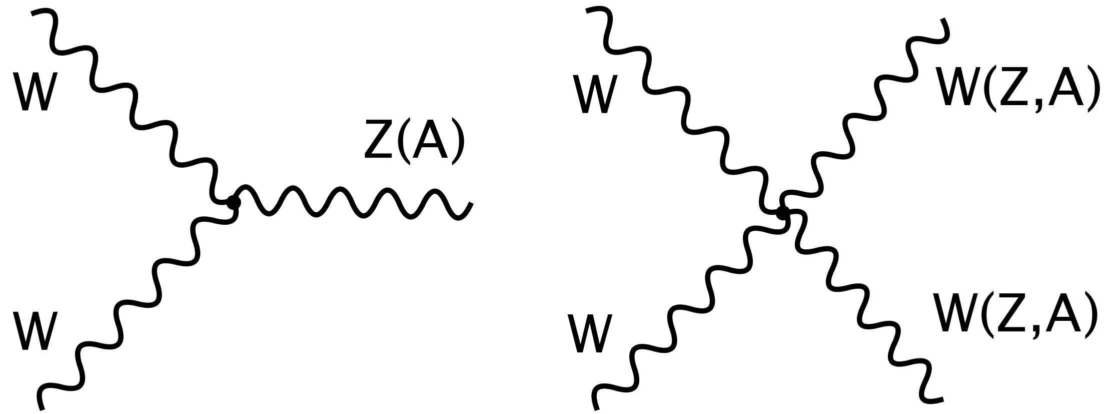


- Trilinear couplings: checking the non-abelian gauge structure.

# SM trilinear and quartic gauge couplings

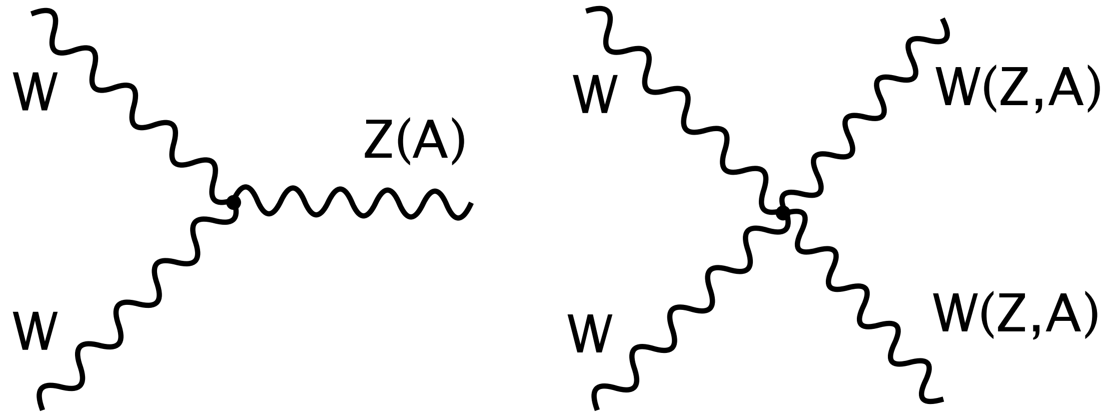


- Trilinear couplings: checking the non-abelian gauge structure.
- Quartic couplings: also give a window on the spontaneous symmetry breaking (SSB) mechanism.

# SM trilinear and quartic gauge couplings

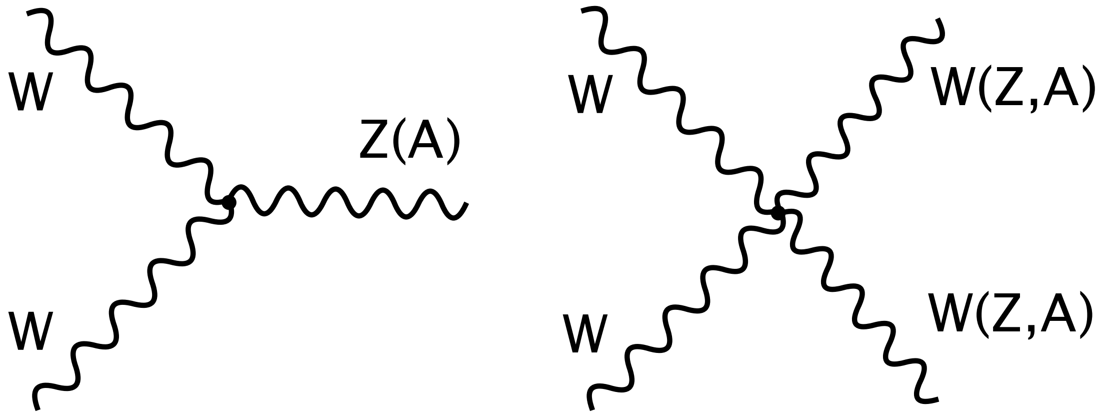


- Trilinear couplings: checking the non-abelian gauge structure.
- Quartic couplings: also give a window on the spontaneous symmetry breaking (SSB) mechanism.
- massive gauge boson scatterings $\rightarrow$ small $M_H$ or new physics at TeV scale.

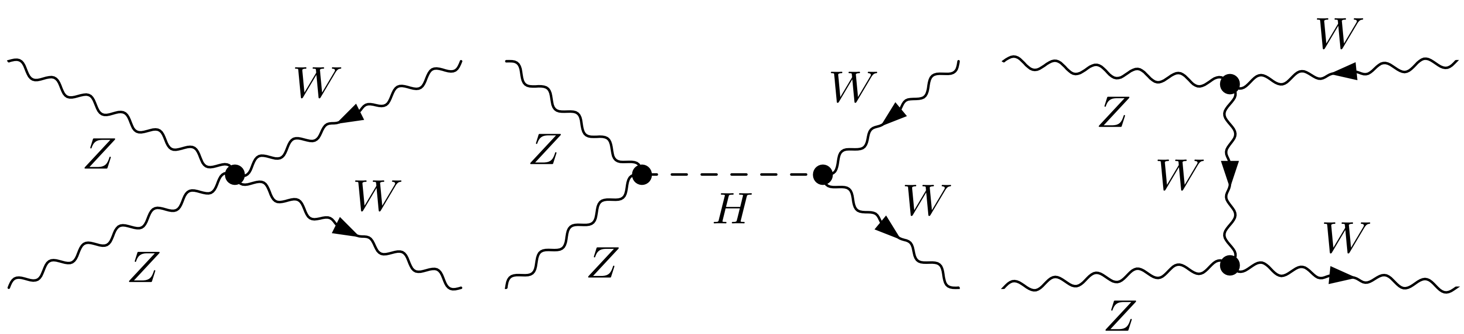


$\Longrightarrow$ this suggests some connection between the Higgs(new physics) and quartic gauge couplings.

# $WW$ production at LEP

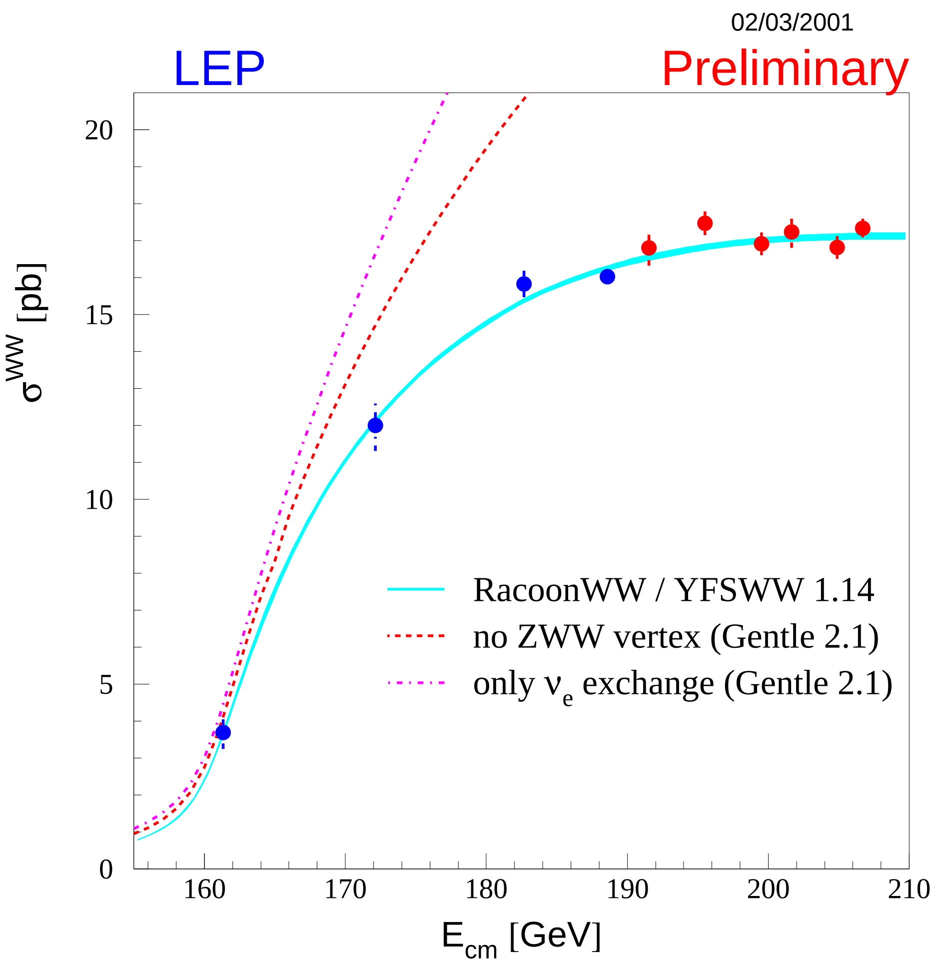


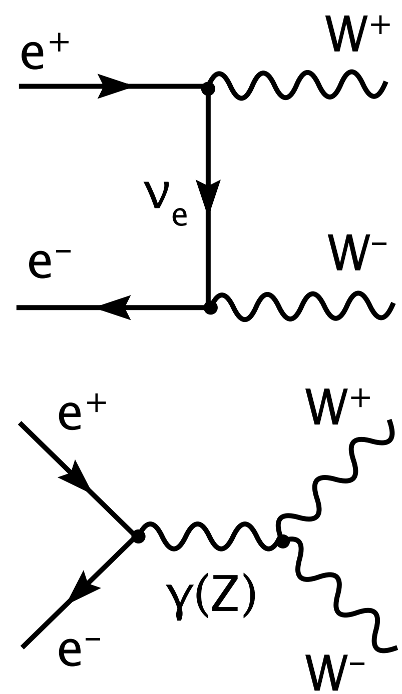


- SM trilinear couplings: well tested at LEP.

# $WW$ production at LEP

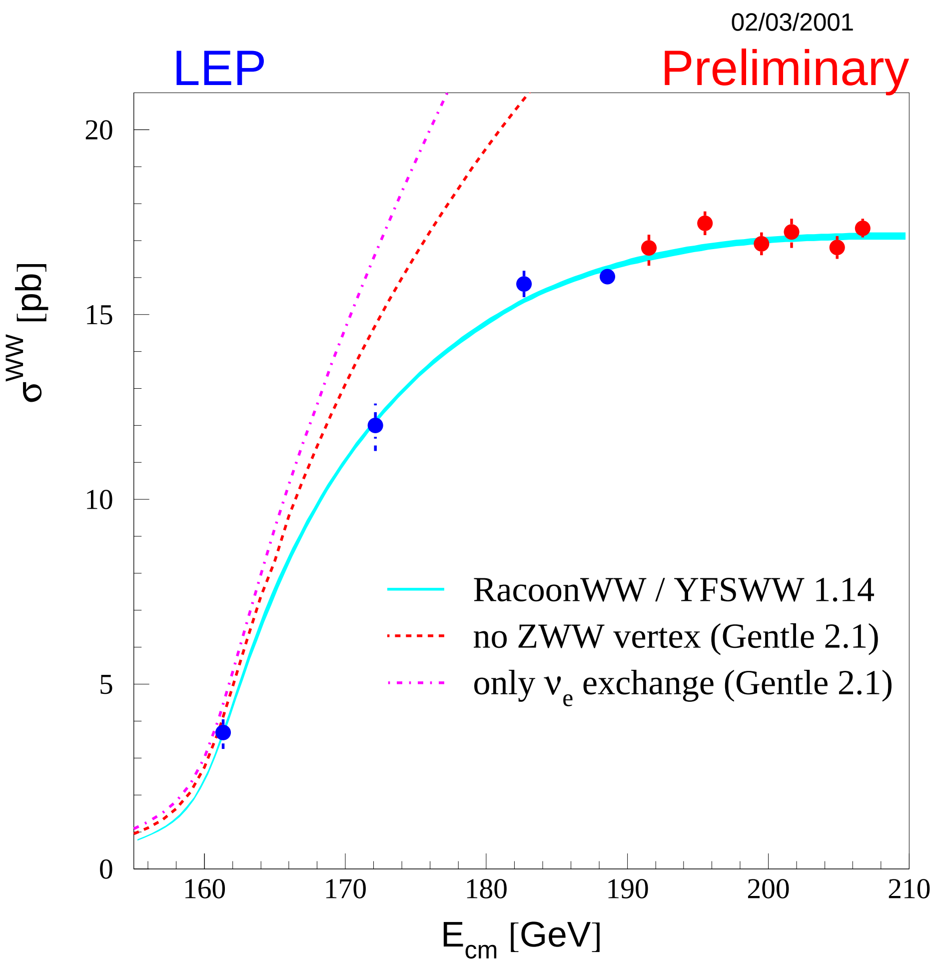


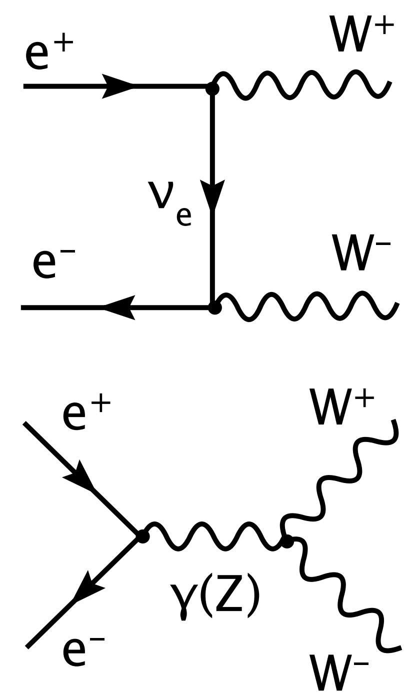


- SM trilinear couplings: well tested at LEP.
- The quartic gauge couplings? Not well tested.

# $e^+e^- \to VVZ$ : tree diagrams

- ZZZ: 9 diagrams, no trilinear and quartic couplings in SM
- WWZ: 20 diagrams, trilinear and quartic couplings contribute in SM

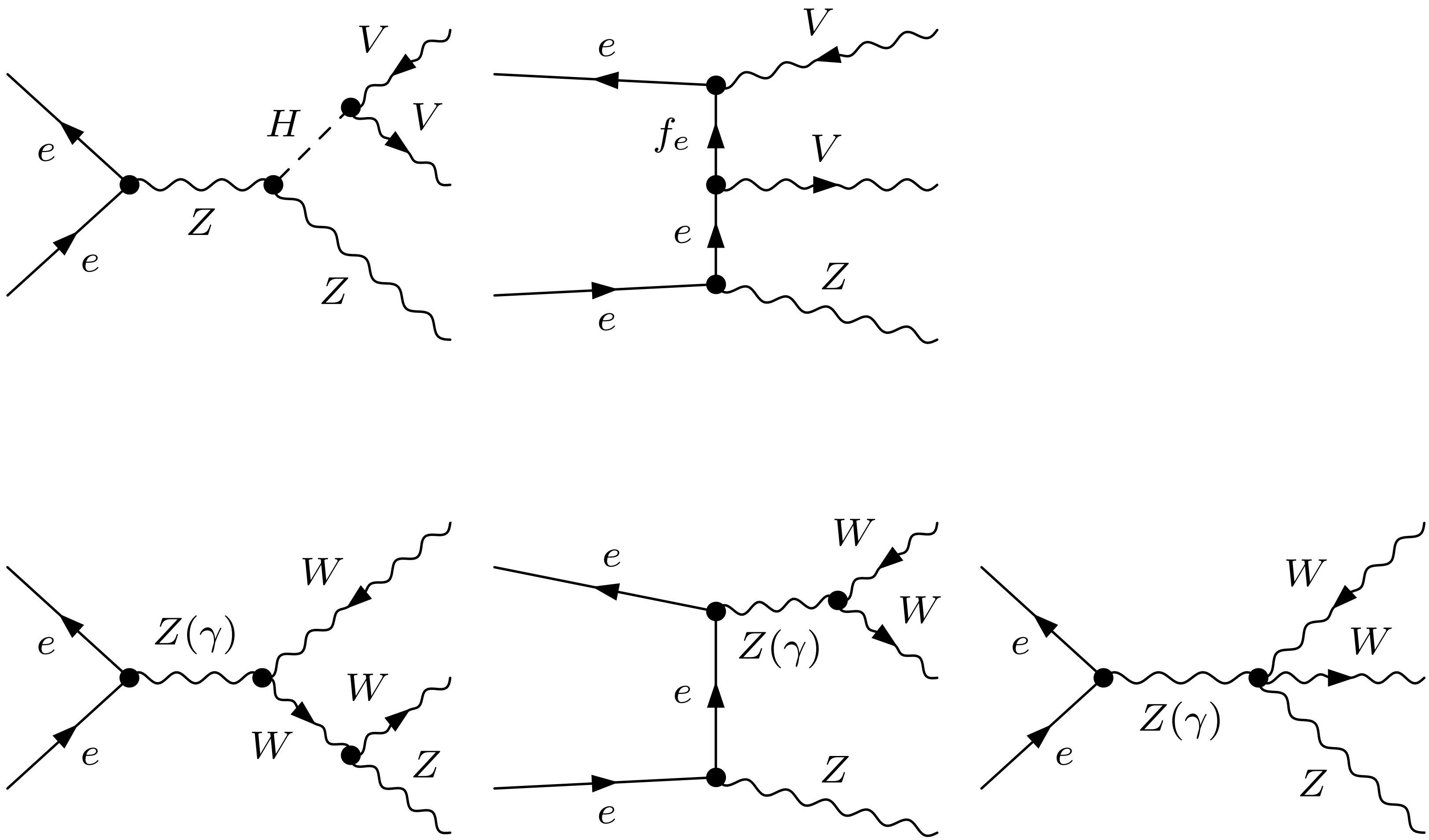

# $e^+e^- \to W^+W^-Z$ : one-loop diagrams

’t Hooft-Feynman guage, neglecting $< eeS >$ couplings:

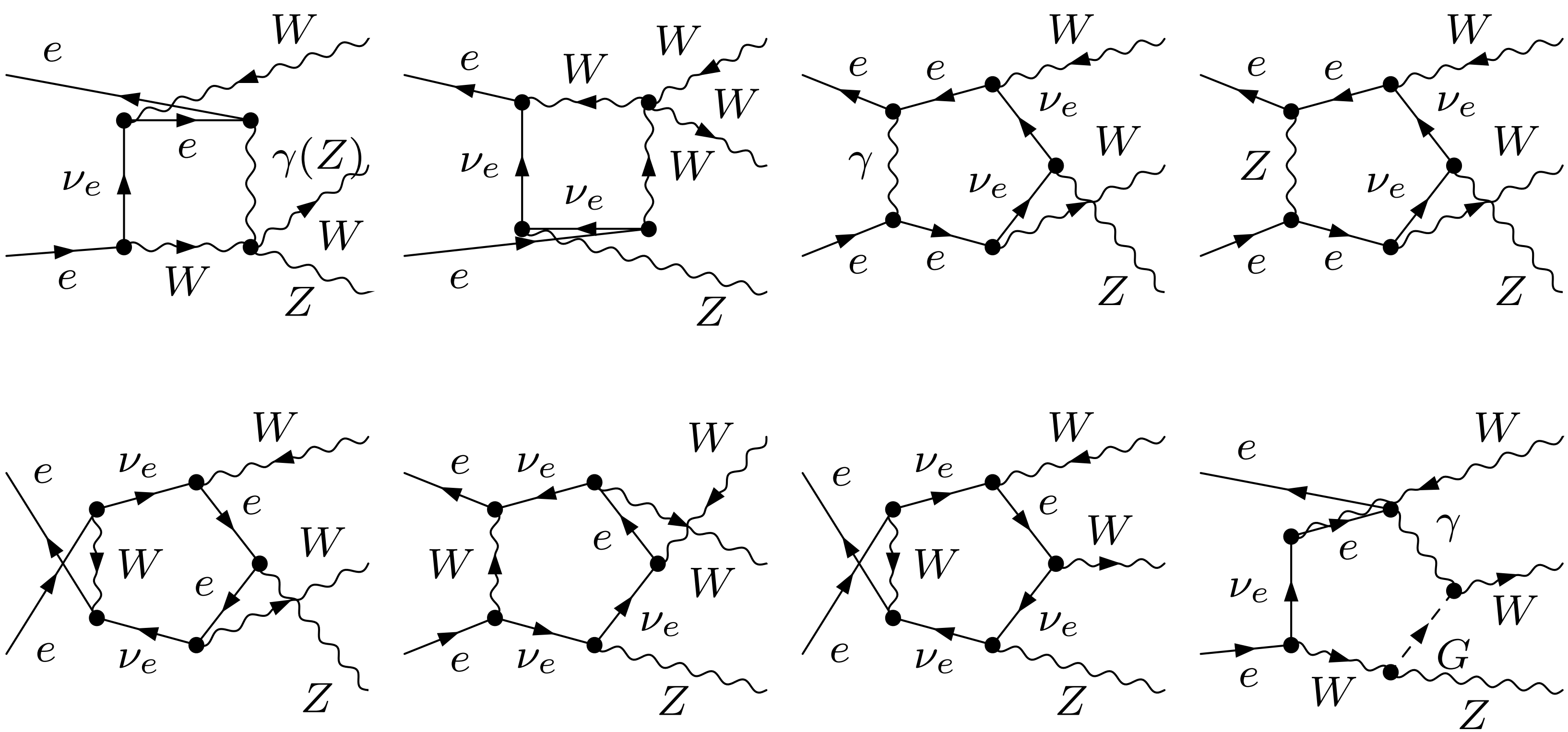


| Topology | $ZZZ(1767)$ | $WWZ(2736)$ |
|---|---|---|
| Loop Amp. (`FormCalc-6.0`) | $6.4$MB | $6.9$MB |
| 4-point | $384$ | $396$ |
| 5-point | $64$ | $109$ |

# General issues in 1-loop multi-leg calculations

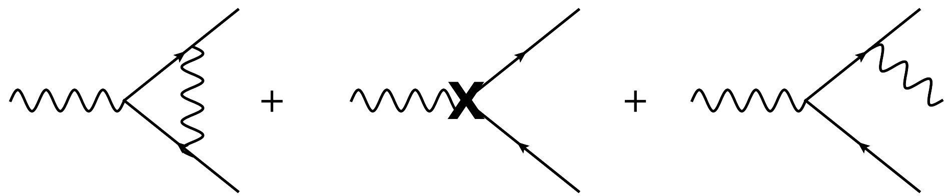

$$d\sigma_{NLO} = d\sigma_{virt} + d\sigma_{real}$$

# General issues in 1-loop multi-leg calculations

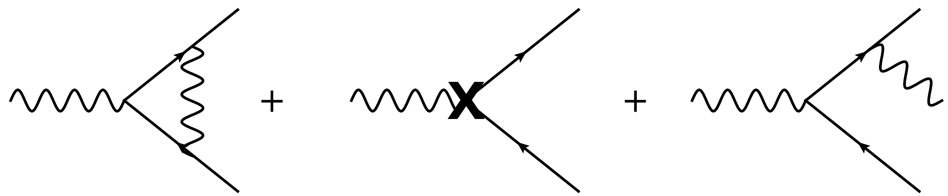

$$d\sigma_{NLO} = d\sigma_{virt} + d\sigma_{real}$$

Physical issues:

- At NLO, many divergences appear: UV, IR, collinear and Landau singularities (pinch singularities in massive loops, EW corrections and unstable particles).

# General issues in 1-loop multi-leg calculations

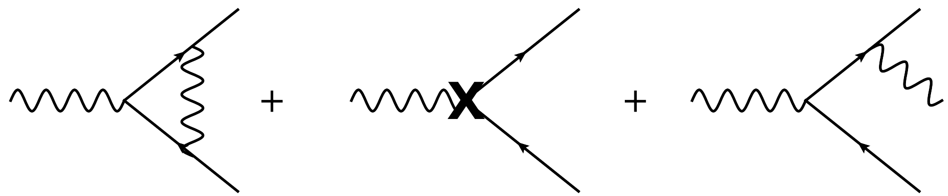

$$d\sigma_{NLO} = d\sigma_{virt} + d\sigma_{real}$$

Physical issues:

- At NLO, many divergences appear: UV, IR, collinear and Landau singularities (pinch singularities in massive loops, EW corrections and unstable particles).

Technical issues:

- Amplitude expressions are very large.
- Numerical instabilities.

# One-loop Renormalisation

UV-divergence is regularised by the means of renormalisation.

- Independent parameters (CKM $= 1$): $e$, $m_f$, $M_W$, $M_Z$, $M_H$
- Renormalized parameters: $e_0 = Z_e e$, $M_0 = M + \delta M$
- Field renormalisation: $\phi_i^0 = (\delta_{ij} + \delta Z_{ij}^{\phi}/2)\phi_i$

# One-loop Renormalisation

UV-divergence is regularised by the means of renormalisation.

- Independent parameters (CKM $= 1$): $e$, $m_f$, $M_W$, $M_Z$, $M_H$
- Renormalized parameters: $e_0 = Z_e e$, $M_0 = M + \delta M$
- Field renormalisation: $\phi_i^0 = (\delta_{ij} + \delta Z_{ij}^{\phi}/2)\phi_i$
- On-shell scheme:
  - All physical masses are the pole positions of the propagator.
  - Field renormalisation: the pole residue is equal to 1, no mixing between on-shell physical fields.
  - $\rightsquigarrow$ The matrix $\delta Z_{ij}^{\phi}$ is, in general, real (CP conserving) but not orthogonal ($\delta Z_{ij}^{\phi} \neq \delta Z_{ji}^{\phi}$).

# One-loop Renormalisation

UV-divergence is regularised by the means of renormalisation.

- Independent parameters (CKM $= 1$): $e$, $m_f$, $M_W$, $M_Z$, $M_H$
- Renormalized parameters: $e_0 = Z_e e$, $M_0 = M + \delta M$
- Field renormalisation: $\phi_i^0 = (\delta_{ij} + \delta Z_{ij}^{\phi}/2)\phi_i$
- On-shell scheme:
  - All physical masses are the pole positions of the propagator.
  - Field renormalisation: the pole residue is equal to 1, no mixing between on-shell physical fields.
  - $\rightsquigarrow$ The matrix $\delta Z_{ij}^{\phi}$ is, in general, real (CP conserving) but not orthogonal ($\delta Z_{ij}^{\phi} \neq \delta Z_{ji}^{\phi}$).
- For the SM, the OS scheme works so well because all the physical masses are independent parameters and hence can be renormalized as the pole positions of the propagator.
  This is not true for the MSSM ($M_{H^\pm}^2 = M_A^2 + M_W^2$).

# Loop integrals and numerical instabilities

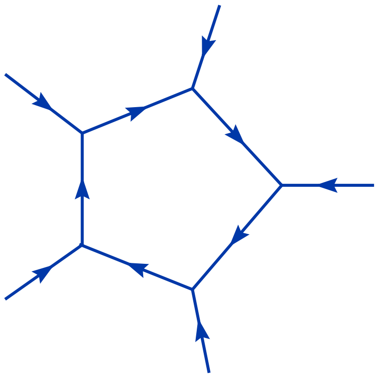

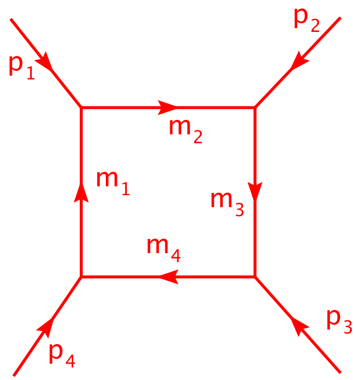


- $k_i = \sum_{j=1}^{i-1} p_j$, $i = 1, 2, 3, \ldots$
- $\det(G) = \det(2k_i \cdot k_j)$: Gram determinant
- $\det(Y) = \det(m_i^2 + m_j^2 - (k_i - k_j)^2)$: Landau determinant

# Loop integrals and numerical instabilities

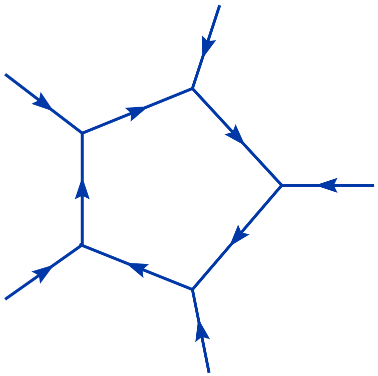

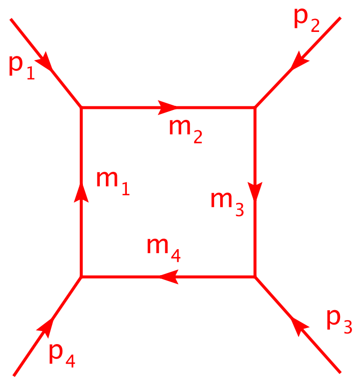


- $k_i = \sum_{j=1}^{i-1} p_j$, $i = 1, 2, 3, \ldots$
- $\det(G) = \det(2k_i \cdot k_j)$: Gram determinant
- $\det(Y) = \det(m_i^2 + m_j^2 - (k_i - k_j)^2)$: Landau determinant
- 5pt integrals are reduced to 4pts Denner and Dittmaier 2002
  $E_0 = -\sum_{i=1}^{5} \frac{\det(Y_i)}{\det(Y)} D_0(i)$

# Loop integrals and numerical instabilities

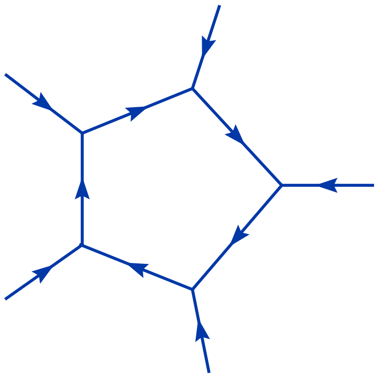

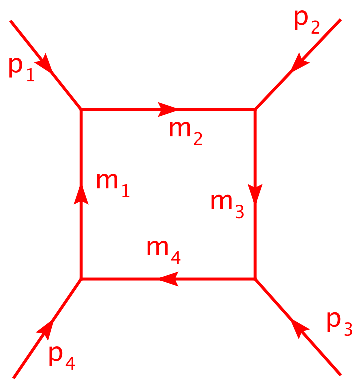


- $k_i = \sum_{j=1}^{i-1} p_j$, $i = 1, 2, 3, \ldots$
- $\det(G) = \det(2k_i \cdot k_j)$: Gram determinant
- $\det(Y) = \det(m_i^2 + m_j^2 - (k_i - k_j)^2)$: Landau determinant

- 5pt integrals are reduced to 4pts Denner and Dittmaier 2002
  $E_0 = -\sum_{i=1}^{5} \frac{\det(Y_i)}{\det(Y)} D_0(i)$
- Tensor 4pt integrals up to rank 4: Passarino-Veltman reduction

$$D_{ijkl} \;=\; f(p_i, m_i)/\det(G)^4$$

$\Longrightarrow$ numerical instabilities occur when $\det(G)$ is small (close to PS boundary).

# Loop integrals and numerical instabilities

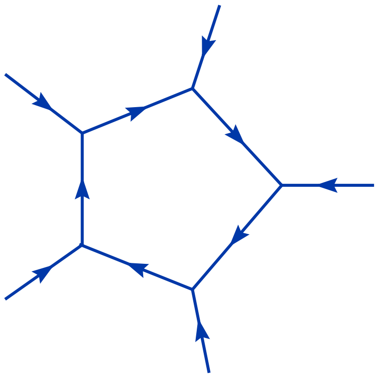

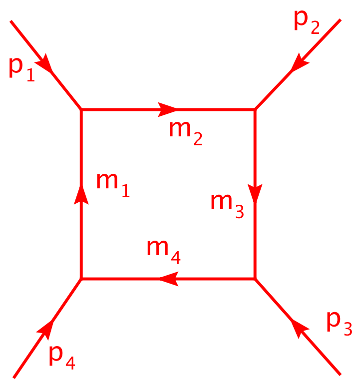


- $k_i = \sum_{j=1}^{i-1} p_j$, $i = 1, 2, 3, \ldots$
- $\det(G) = \det(2k_i \cdot k_j)$: Gram determinant
- $\det(Y) = \det(m_i^2 + m_j^2 - (k_i - k_j)^2)$: Landau determinant

- 5pt integrals are reduced to 4pts Denner and Dittmaier 2002
  $E_0 = -\sum_{i=1}^{5} \frac{\det(Y_i)}{\det(Y)} D_0(i)$
- Tensor 4pt integrals up to rank 4: Passarino-Veltman reduction

$$D_{ijkl} \;=\; f(p_i, m_i)/\det(G)^4$$

$\Longrightarrow$ numerical instabilities occur when $\det(G)$ is small (close to PS boundary).

- Our solutions: small DetG expansion or using quadruple precision (loop library only, the results become stable, 6 times slower).

# Loop integrals and numerical instabilities

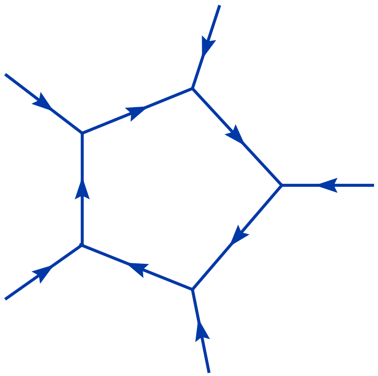

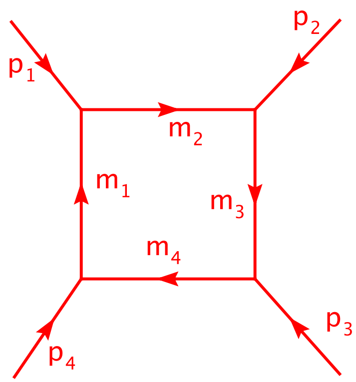


- $k_i = \sum_{j=1}^{i-1} p_j,\, i = 1, 2, 3, \ldots$
- $\det(G) = \det(2k_i \cdot k_j)$: Gram determinant
- $\det(Y) = \det(m_i^2 + m_j^2 - (k_i - k_j)^2)$: Landau determinant

- 5pt integrals are reduced to 4pts Denner and Dittmaier 2002
  $E_0 = -\sum_{i=1}^{5} \frac{\det(Y_i)}{\det(Y)} D_0(i)$
- Tensor 4pt integrals up to rank 4: Passarino-Veltman reduction

$$\boxed{D_{ijkl} \;=\; f(p_i, m_i)/\det(G)^4}$$

  $\Longrightarrow$ numerical instabilities occur when $\det(G)$ is small (close to PS boundary).
- Our solutions: small DetG expansion or using quadruple precision (loop library only, the results become stable, 6 times slower).
- Scalar 4pt integrals can also have numerical cancellation (observed in WWZ):
  - Using different methods (projective transformation, 't Hooft and Veltman 1979, is good for $m_i = 0$; direct calculation for $p_j^2 = 0$).
  - Using quadruple precision helps.

# Real correction

$$d\sigma_{1-loop}^{e^+e^-\to VVZ} = d\sigma_{virt}^{e^+e^-\to VVZ} + d\sigma_{real}^{e^+e^-\to VVZ\gamma}$$

- The virtual part contains both soft and collinear divergences. All these singularities are cancelled by adding the real photon radiation process.

# Real correction

$$d\sigma_{1-loop}^{e^+e^-\to VVZ} = d\sigma_{virt}^{e^+e^-\to VVZ} + d\sigma_{real}^{e^+e^-\to VVZ\gamma}$$

- The virtual part contains both soft and collinear divergences. All these singularities are cancelled by adding the real photon radiation process.
- All singularities in the real amplitude can be factorised, $P_{ff}(y) = (1+y^2)/(1-y)$:

$$\sum_{\lambda_\gamma} |M_1|^2 \quad \widetilde{k\to 0} \quad -\sum_{f,f'} Q_f\sigma_f Q_{f'}\sigma_{f'} e^2 \frac{p_f p_{f'}}{(p_f k)(p_{f'} k)} |M_0|^2,$$

$$\sum_{\lambda_\gamma} |M_1|^2 \quad \widetilde{p_i k\to 0} \quad Q_i^2 e^2 \frac{1}{p_i k}\left[P_{ff}(z_i) - \frac{m_i^2}{p_i k}\right] |M_0(p_i + k)|^2,$$

$$\sum_{\lambda_\gamma} |M_1|^2 \quad \widetilde{p_a k\to 0} \quad Q_a^2 e^2 \frac{1}{x_a(p_a k)}\left[P_{ff}(x_a) - \frac{x_a m_a^2}{p_a k}\right] |M_0(x_a p_a)|^2.$$

# Real correction

$$d\sigma_{1-loop}^{e^+e^-\to VVZ} = d\sigma_{virt}^{e^+e^-\to VVZ} + d\sigma_{real}^{e^+e^-\to VVZ\gamma}$$

- The virtual part contains both soft and collinear divergences. All these singularities are cancelled by adding the real photon radiation process.
- All singularities in the real amplitude can be factorised, $P_{ff}(y) = (1+y^2)/(1-y)$:

$$\sum_{\lambda_\gamma} |M_1|^2 \quad \widetilde{k\to 0} \quad -\sum_{f,f'} Q_f\sigma_f Q_{f'}\sigma_{f'} e^2 \frac{p_f p_{f'}}{(p_f k)(p_{f'} k)} |M_0|^2,$$

$$\sum_{\lambda_\gamma} |M_1|^2 \quad \widetilde{p_i k\to 0} \quad Q_i^2 e^2 \frac{1}{p_i k}\left[P_{ff}(z_i) - \frac{m_i^2}{p_i k}\right] |M_0(p_i+k)|^2,$$

$$\sum_{\lambda_\gamma} |M_1|^2 \quad \widetilde{p_a k\to 0} \quad Q_a^2 e^2 \frac{1}{x_a(p_a k)}\left[P_{ff}(x_a) - \frac{x_a m_a^2}{p_a k}\right] |M_0(x_a p_a)|^2.$$

- After adding the virtual and real corrections the result is still collinear singular. This singularity comes from the initial state radiation part, in the form $\alpha \ln(s/m_e^2)$ after int.

# Real correction

$$d\sigma_{1-loop}^{e^+e^-\to VVZ} = d\sigma_{virt}^{e^+e^-\to VVZ} + d\sigma_{real}^{e^+e^-\to VVZ\gamma}$$

- The virtual part contains both soft and collinear divergences. All these singularities are cancelled by adding the real photon radiation process.
- All singularities in the real amplitude can be factorised, $P_{ff}(y) = (1+y^2)/(1-y)$:

$$\sum_{\lambda_\gamma} |M_1|^2 \quad \widetilde{k\to 0} \quad -\sum_{f,f'} Q_f\sigma_f Q_{f'}\sigma_{f'} e^2 \frac{p_f p_{f'}}{(p_f k)(p_{f'}k)} |M_0|^2,$$

$$\sum_{\lambda_\gamma} |M_1|^2 \quad \widetilde{p_i k\to 0} \quad Q_i^2 e^2 \frac{1}{p_i k}\left[P_{ff}(z_i) - \frac{m_i^2}{p_i k}\right] |M_0(p_i + k)|^2,$$

$$\sum_{\lambda_\gamma} |M_1|^2 \quad \widetilde{p_a k\to 0} \quad Q_a^2 e^2 \frac{1}{x_a(p_a k)}\left[P_{ff}(x_a) - \frac{x_a m_a^2}{p_a k}\right] |M_0(x_a p_a)|^2.$$

- After adding the virtual and real corrections the result is still collinear singular. This singularity comes from the initial state radiation part, in the form $\alpha \ln(s/m_e^2)$ after int.
- Two ways to calculate: phase space slicing and subtraction methods.

# Real correction: phase space slicing

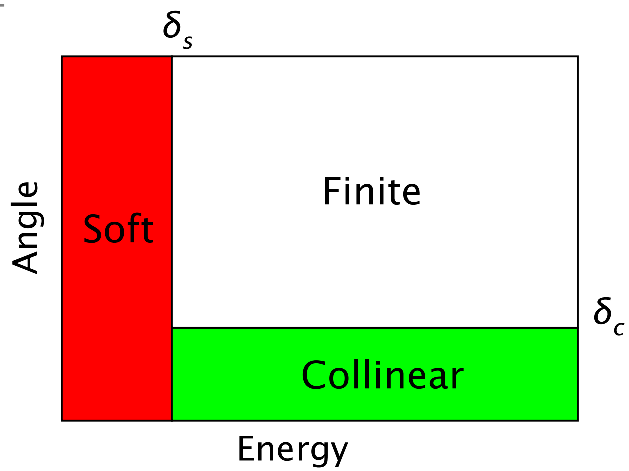


- Real correction is cutoff-independent.
- Factorization condition: $\delta_s$ and $\delta_c$ are sufficiently small. And $\delta_c \gg 2m_e^2/s$ to use the collinear integration formula.

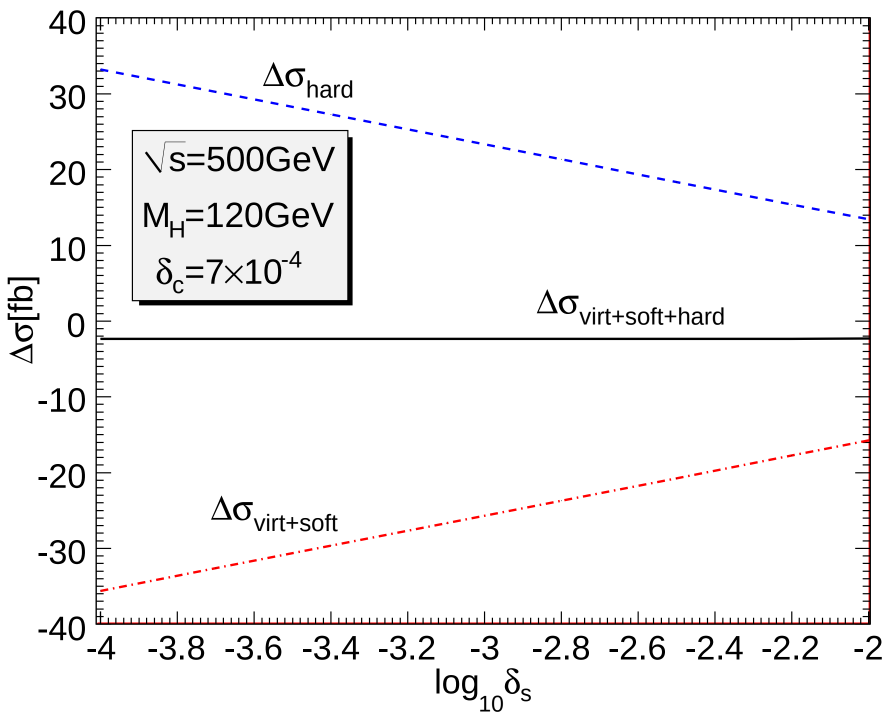


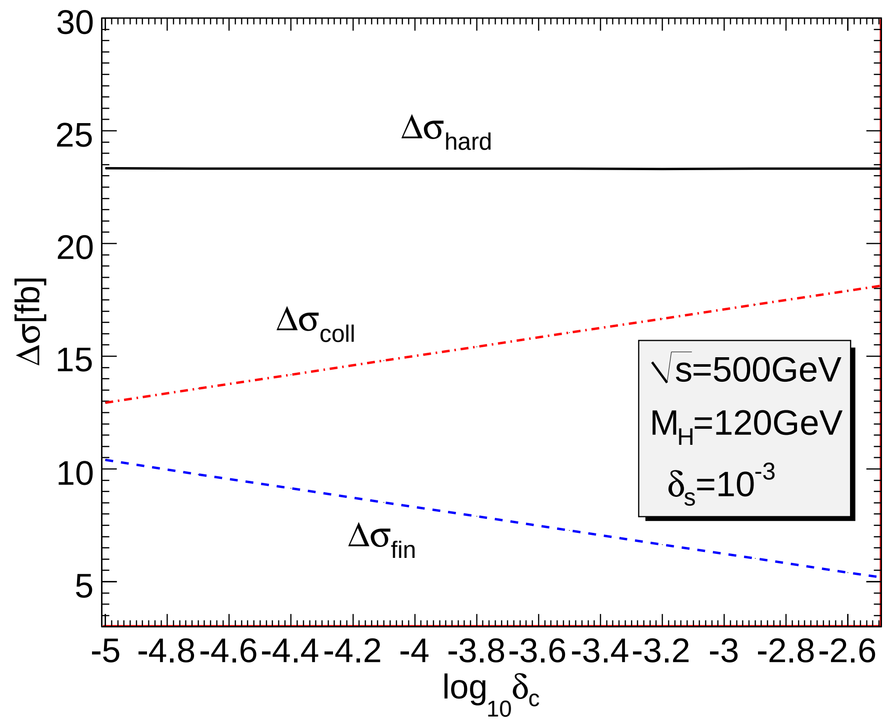

# Real correction: dipole subtraction

$$\sigma_{\text{real}} = \int_4 (\mathrm{d}\sigma_{\text{real}} - \mathrm{d}\sigma_{\text{sub}}) + \int_4 \mathrm{d}\sigma_{\text{sub}}.$$

The subtraction function should be:

- the same as the real function $\mathrm{d}\sigma_{\text{real}}$ in the singular limits.
- simple enough so that it can be analytically integrated over the singular region.

The dipole subtraction method Catani, Seymour, Dittmaier ...:

$$\int_4 \mathrm{d}\sigma_{\text{sub}} = -\frac{\alpha}{2\pi} \int \mathrm{d}x \sum_{i\neq j} Q_i Q_j \, \mathcal{G}_{ij}(x) \int_3 \mathrm{d}\sigma_{\text{Born}} + \sigma_{\text{endpoint}},$$

$$\sigma_{\text{endpoint}} = -\frac{\alpha}{2\pi} \int_3 \mathrm{d}\sigma_{\text{Born}} \sum_{i\neq j} Q_i Q_j \, G_{ij}.$$

- The subtraction function is a sum of many dipole terms.
- The endpoint contribution contains all the soft and collinear singularities of the virtual part, with the opposite signs:

$$\boxed{\sigma_{\text{weak}} = \sigma_{\text{virt}} + \sigma_{\text{endpoint}}: \text{ soft and coll. finite}}$$

# Real correction: dipole vs. slicing

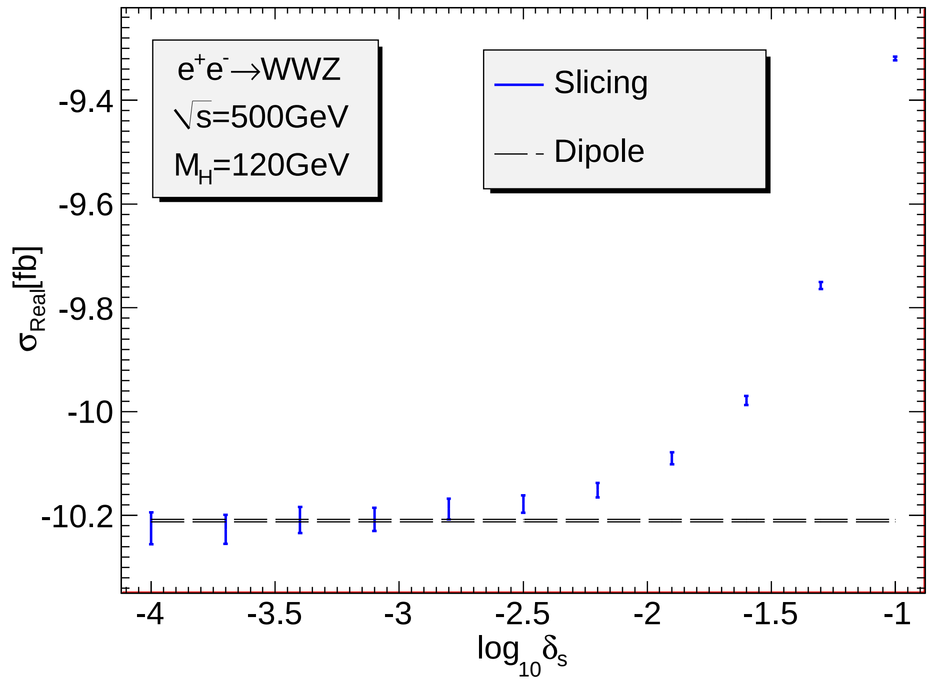


- Slicing: simple, easy to implement, large integration error. We use this to cross check the results.
  Tricky point: when one decreases the error, the cut-offs must also be reduced.
- Dipole: subtraction function is quite complicated (not so easy to implement), the integration error is typically 10 times smaller than slicing's, no cut-off dependence.
  Tricky point: misbinning effect in histograms.
- Calculating real correction is more time-consuming than getting the virtual part.

# Amplitude factorization

Helicity loop for $e^+e^- \to W^+W^-Z$:

```
do λ_{e^-} = -1, 1
  do λ_{e^+} = -1, 1
    do λ_{W^-} = -1, 0, 1
      do λ_{W^+} = -1, 0, 1
        do λ_Z = -1, 0, 1
          call A(λ_{e^-}, λ_{e^+}, λ_{W^-}, λ_{W^+}, λ_Z)
        enddo
      ...
```

do $\lambda_{e^-} = -1, 1$

do $\lambda_{e^+} = -1, 1$

do $\lambda_{W^-} = -1, 0, 1$

do $\lambda_{W^+} = -1, 0, 1$

do $\lambda_Z = -1, 0, 1$

**call** $\mathcal{A}(\lambda_{e^-}, \lambda_{e^+}, \lambda_{W^-}, \lambda_{W^+}, \lambda_Z)$

enddo

...

# Amplitude factorization

Helicity loop for $e^+e^- \to W^+W^-Z$:

do $\lambda_{e^-} = -1, 1$

do $\lambda_{e^+} = -1, 1$

do $\lambda_{W^-} = -1, 0, 1$

do $\lambda_{W^+} = -1, 0, 1$

do $\lambda_Z = -1, 0, 1$

**call** $\mathcal{A}(\lambda_{e^-}, \lambda_{e^+}, \lambda_{W^-}, \lambda_{W^+}, \lambda_Z)$

enddo

...

Factorization:

$$\mathcal{A} = Const \times SME(\lambda_i, p_i) \times FF(p_i, m_j).$$

# Amplitude factorization

Helicity loop for $e^+e^- \to W^+W^-Z$:

do $\lambda_{e^-} = -1, 1$

do $\lambda_{e^+} = -1, 1$

do $\lambda_{W^-} = -1, 0, 1$

do $\lambda_{W^+} = -1, 0, 1$

do $\lambda_Z = -1, 0, 1$

**call** $\mathcal{A}(\lambda_{e^-}, \lambda_{e^+}, \lambda_{W^-}, \lambda_{W^+}, \lambda_Z)$

enddo

...

Factorization:

$$\mathcal{A} = Const \times SME(\lambda_i, p_i) \times FF(p_i, m_j).$$

- $FF(p_i, m_j)$: a linear combination of loop integrals, very large expressions (`FORM` complains!). $FF$s appear several times and are put in the common block.

# Amplitude factorization

Helicity loop for $e^+e^- \to W^+W^-Z$:

do $\lambda_{e^-} = -1, 1$

  do $\lambda_{e^+} = -1, 1$

    do $\lambda_{W^-} = -1, 0, 1$

      do $\lambda_{W^+} = -1, 0, 1$

        do $\lambda_Z = -1, 0, 1$

          **call** $\mathcal{A}(\lambda_{e^-}, \lambda_{e^+}, \lambda_{W^-}, \lambda_{W^+}, \lambda_Z)$

        enddo

      ...

Factorization:

$$\mathcal{A} = Const \times SME(\lambda_i, p_i) \times FF(p_i, m_j).$$

- $FF(p_i, m_j)$: a linear combination of loop integrals, very large expressions (`FORM` complains!). $FF$s appear several times and are put in the common block.
- Solution: divide into small groups of Feynman diagrams.

# Amplitude factorization

Helicity loop for $e^+e^- \to W^+W^-Z$:

do $\lambda_{e^-} = -1, 1$

  do $\lambda_{e^+} = -1, 1$

    do $\lambda_{W^-} = -1, 0, 1$

      do $\lambda_{W^+} = -1, 0, 1$

        do $\lambda_Z = -1, 0, 1$

          **call** $\mathcal{A}(\lambda_{e^-}, \lambda_{e^+}, \lambda_{W^-}, \lambda_{W^+}, \lambda_Z)$

        enddo

      ...

Factorization:

$$\mathcal{A} = Const \times SME(\lambda_i, p_i) \times FF(p_i, m_j).$$

- $FF(p_i, m_j)$: a linear combination of loop integrals, very large expressions (`FORM` complains!). $FF$s appear several times and are put in the common block.
- Solution: divide into small groups of Feynman diagrams.
- The calculation is about 2 times faster than the normal `FormCalc-6.0`(already optimized by introducing many abbreviations).

# Checks on the results

- Non-linear gauge (NLG) invariance check: tree and one-loop squared amplitude level. We use `SloopS`(Baro, Boudjema and Semenov; `FeynArts`+NLG).
- The results should be UV and IR finite.
- Loop integrals: tricky part, use different codes (methods) to cross check. `LoopTools`/FF(van Oldenborgh, Hahn), `OneLOop`(van Hameren), `D0C`(D. T. Nhung, LDN; D0 with complex masses; adapted version in `LoopTools-2.n`, $n > 3$). Link: http://wwwth.mppmu.mpg.de/members/ldninh/index.html
- Phase space integration: (parallel) BASES, VEGAS.
- Two independent calculations (codes): Fortran 77, C++; generated with the help of `FeynArts-3.4`, `FormCalc-6.0`(Math + FORM).
- Comparisons with other groups (more later).

# NLG Check and numerical instability

NLG fixing Lagrangian (Boudjema, Chopin 1995):

$$\mathcal{L}_{GF} = -\frac{1}{\xi_W}|(\partial_\mu - ie\tilde{\alpha}A_\mu - igc_W\tilde{\beta}Z_\mu)W^{\mu+} + \xi_W\frac{g}{2}(v+\tilde{\delta}H + i\tilde{\kappa}\chi_3)\chi^+|^2$$
$$-\frac{1}{2\xi_Z}(\partial.Z + \xi_Z\frac{g}{2c_W}(v+\tilde{\varepsilon}H)\chi_3)^2 - \frac{1}{2\xi_A}(\partial.A)^2 \,.$$

| $(\tilde{\alpha}, \tilde{\beta})$ | ZZZ | WWZ(1) | WWZ(2) |
|---|---|---|---|
| (0,0) | -7.8077709362570481E-4 | -6.3768793214220439E-2 | 5.58809251111264704781982030672 7217E-2 |
| (1,0) | -7.8077709362570731E-4 | -6.3767676883630841E-2 | 5.5880925111110349911426963080135 26E-2 |
| (0,1) | -7.8077709361534624E-4 | -6.3772289648961160E-2 | 5.5880925111146084510166105297238 1E-2 |

- $ZZZ$: at least 10 digit agreement with double precision (DP).
- $WWZ$: 4 digits with DP, 12 digits with quadruple precision.
  $\rightsquigarrow$ This is an indication of numerical instability.

# Comparisons for $ZZZ$

| $\sqrt{s}$ [GeV] | | $M_H = 120$GeV $\sigma_{Born}$[fb] | $M_H = 120$GeV $\delta_{full}$ [%] | $M_H = 150$GeV $\sigma_{Born}$[fb] | $M_H = 150$GeV $\delta_{full}$ [%] |
|---|---|---|---|---|---|
| 350 | Ref. [1] | 0.58696 | -15.79 | 0.68422 | -13.91 |
| | This work | 0.586955(2) | -15.850(1) | 0.684209(2) | -13.970(1) |
| 400 | Ref. [1] | 0.83409 | -11.75 | 0.9375 | -9.98 |
| | This work | 0.834083(4) | -11.765(2) | 0.937484(4) | -9.973(1) |
| 450 | Ref. [1] | 0.95792 | -9.79 | 1.05294 | -8.06 |
| | This work | 0.957904(5) | -9.763(3) | 1.052917(5) | -8.044(2) |
| 500 | Ref. [1] | 1.01384 | -8.70 | 1.09754 | -7.09 |
| | This work | 1.013806(6) | -8.682(4) | 1.097440(7) | -7.064(4) |
| 600 | Ref. [1] | 1.03052 | -7.77 | 1.09370 | -6.36 |
| | This work | 1.030489(9) | -7.714(6) | 1.093668(9) | -6.289(6) |
| 1000 | Ref. [1] | 0.83892 | -7.94 | 0.86366 | -6.89 |
| | This work | 0.83887(2) | -7.86(2) | 0.86362(2) | -6.86(2) |

[1] Su Ji-Juan, Ma Wen-Gan *et al.*, Phys. Rev. D78, 016007 (2008).

# Comparisons for $WWZ$

| | | $M_H = 120$GeV | | $M_H = 150$GeV | |
|---|---|---|---|---|---|
| $\sqrt{s}$ [TeV] | | $\sigma_{Born}$[fb] | $\Delta\sigma_{NLO}$[fb] | $\sigma_{Born}$[fb] | $\Delta\sigma_{NLO}$[fb] |
| 0.3 | Ref. [2ab] | 3.6216(2) | -0.683(2) | 3.8856(2) | -0.694(2) |
| | This work | 3.62165(5) | -0.6901(3) | 3.88558(5) | -0.7010(3) |
| 0.5 | Ref. [2ab] | 44.026(5) | -3.03(6) | 44.303(5) | -2.89(6) |
| | This work | 44.0235(10) | -3.107(3) | 44.301(1) | -2.949(3) |
| 0.8 | Ref. [2a] | 64.35(1) | -3.48(7) | 64.50(1) | -3.57(9) |
| | Ref. [2b] | 64.35(1) | -3.48(7) | 64.50(1) | -3.11(8) |
| | This work | 64.345(4) | -3.466(8) | 64.488(4) | -3.250(8) |
| 1.0 | Ref. [2a] | 65.42(1) | -3.74(9) | 65.51(1) | -3.90(9) |
| | Ref. [2b] | 65.42(1) | -3.74(9) | 65.51(1) | -3.40(9) |
| | This work | 65.401(5) | -3.650(9) | 65.499(5) | -3.440(10) |

[2a] Sun Wei, Ma Wen-Gan *et al.*, Phys. Lett. B680, 321 (2009).

[2b] Erratum-ibid. 684 (2010) 281.

# $e^+e^- \to ZZZ$: Total Xsection

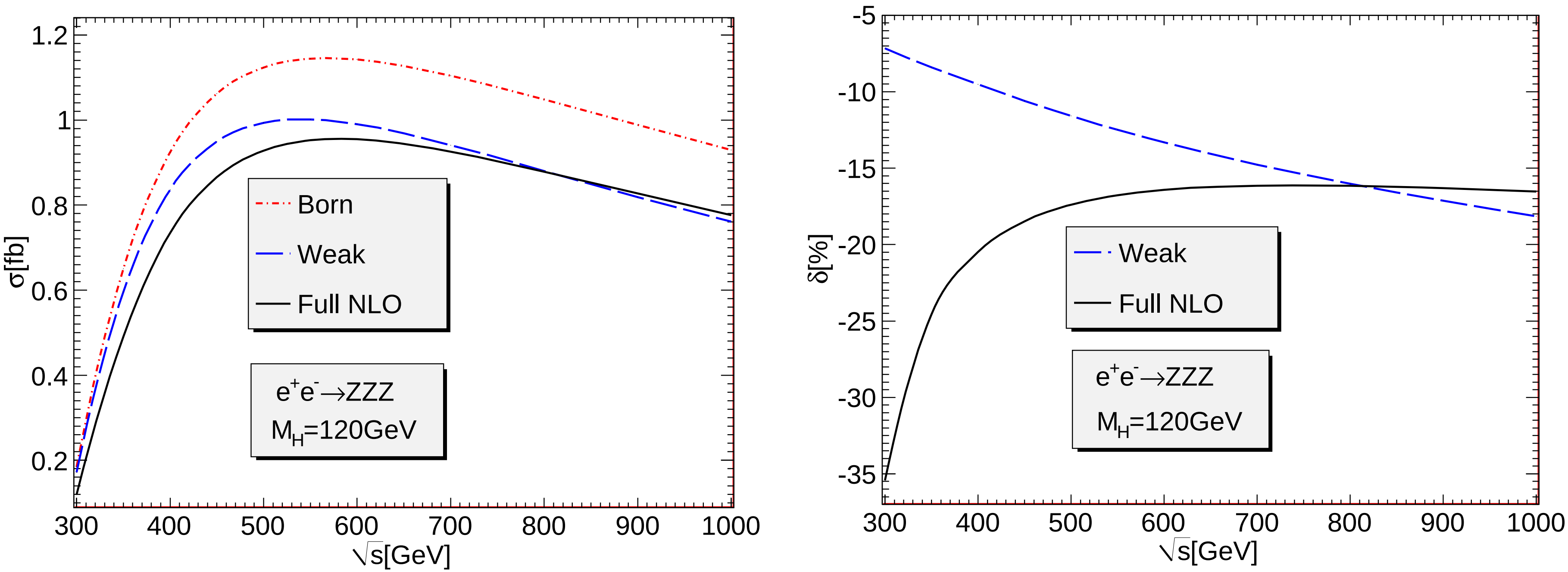


Input parameters: $\alpha_{G_\mu} = \sqrt{2} G_\mu s_W^2 M_W^2/\pi = \alpha(0)(1+\Delta r)$

$$\delta Z_e^{G_\mu} = \delta Z_e - \frac{1}{2}(\Delta r)_{1-\text{loop}}.$$

- Total Xsection peak about $1$fb is at $\sqrt{s} \approx 550$GeV.
- The weak correction goes from $-12\%$ to $-18\%$ when $\sqrt{s}$ increases from $500$GeV to $1$TeV.

# $e^+e^- \to W^+W^-Z$: Total Xsection

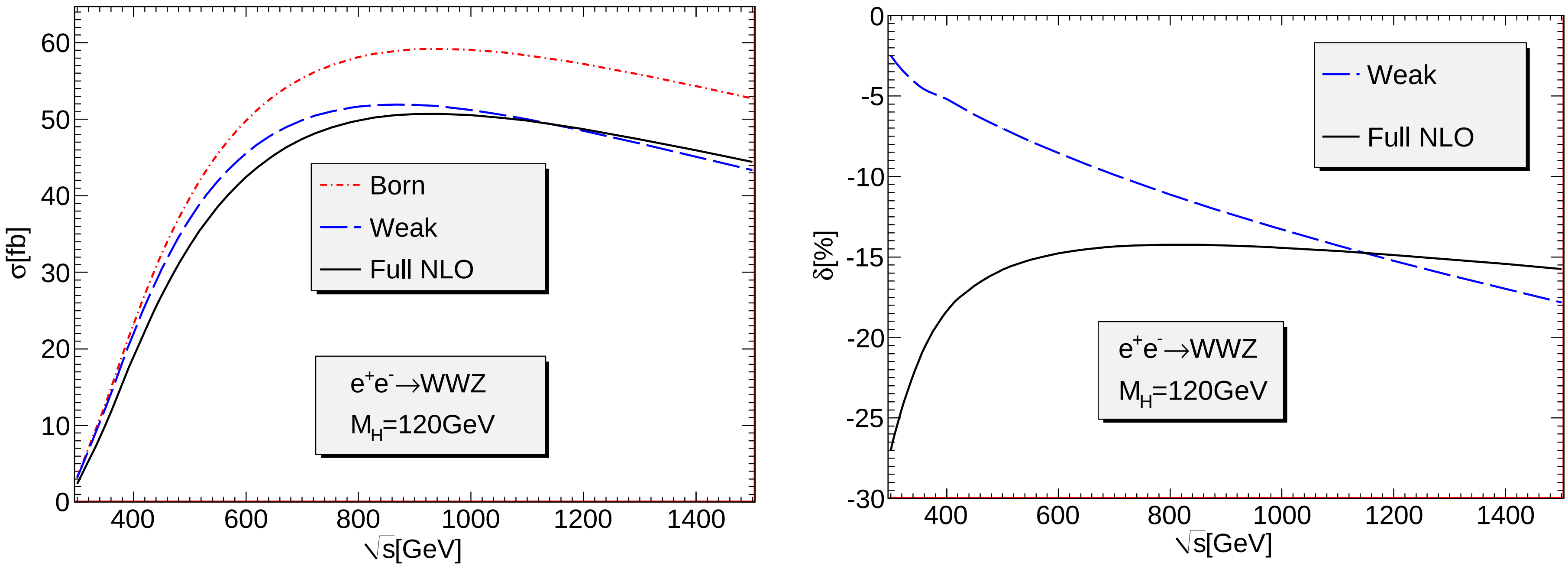


- Total Xsection peak about $50$fb (50 times larger than $\sigma_{ZZZ}$) is at $\sqrt{s} \approx 900$GeV.
- Large Sudakov corrections at high energies: $\alpha \log(M_W^2/s)$, $\alpha \log^2(M_W^2/s)$.
- The weak correction goes from $-7\%$ to $-18\%$ when $\sqrt{s}$ increases from $500$GeV to $1.5$TeV.

# $e^+e^- \to W^+W^-Z$: Distributions (I)

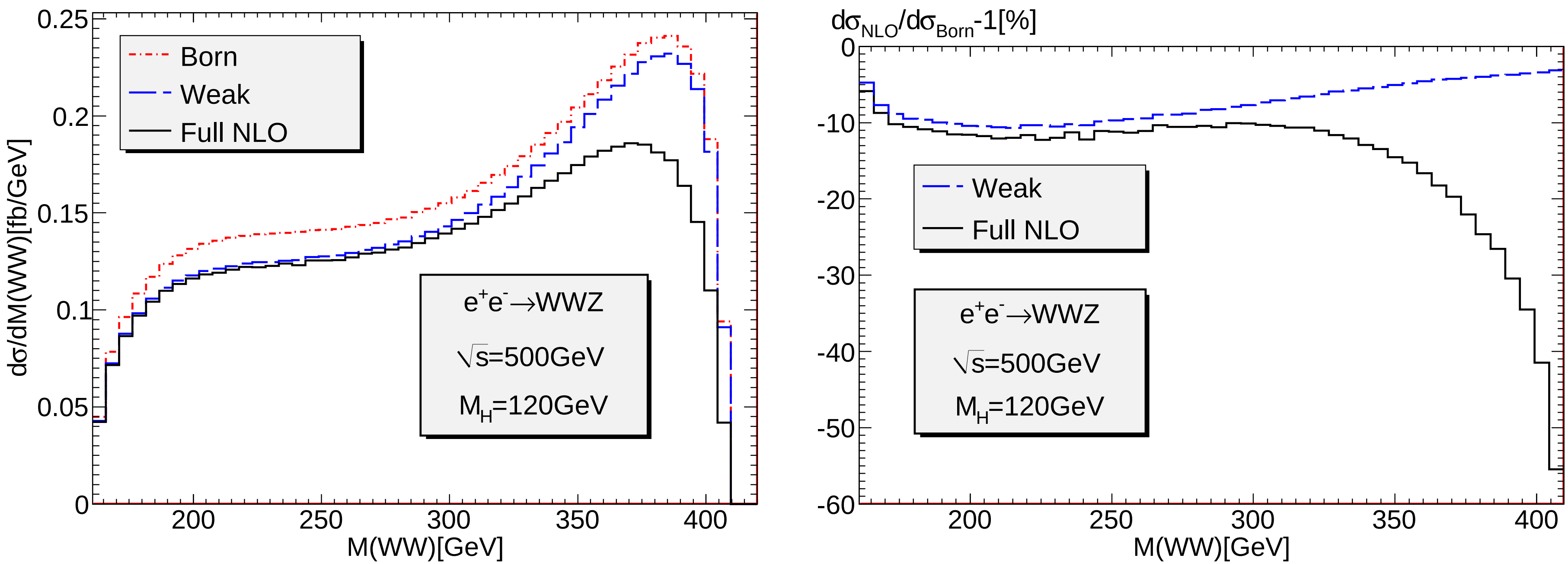


- Quite small corrections (about $-10\%$) at small GeV. At large GeV, large corrections ($-50\%$) due to the hard photon effect [dominant contribution comes from the low-energy photon region which corresponds to large $p_T^Z$ and large $M_{WW}$.]

# $e^+e^- \to W^+W^-Z$: Distributions (II)

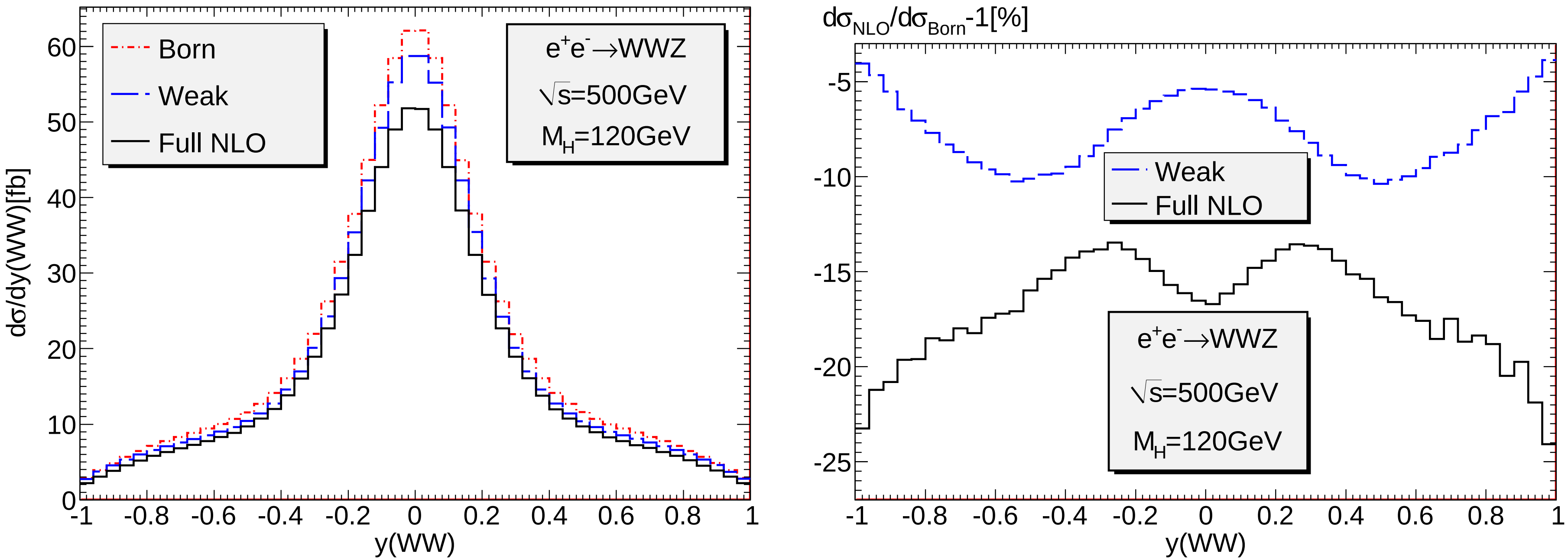


- NLO corrections show new structures, which cannot be explained by an overall scale factor.

# Conclusions

- Tri-boson production (ZZZ and WWZ) at the ILC is an important process to test the quartic gauge couplings and the Higss mechanism. This is the first step towards the understanding of SSB mechanism if the LHC cannot find the Higgs.
- The results indicate that EW corrections are significant and have to be taken into account when doing analysis.
- Our codes (Fortran 77 and C++) can be provided to future experimentalists as a complete library for extensive studies. This can be faster than general-purpose NLO generators.